Tungsten-183 NMR: A Complete and Unequivocal Assignment of the Tungsten–Tungsten Connectivities in Heteropolytungstates via Two-Dimensional ^{183}W NMR Techniques

C. Brevard,*† R. Schimpf,† G. Tourne,‡ and C. M. Tourne‡

Contribution from the Bruker Spectrospin, 34, rue de l'industrie, Boite Postale N, 67160 Wissembourg, France, and Laboratoire de Chimie des Solides, Université des Sciences et Techniques du Languedoc, Place E. Bataillon, 34060 Montpellier, France. *Received March 14, 1983*

Abstract: The importance of polytungstates as model compounds for homogeneous or homogeneous–heterogeneous catalysis is now well recognized, because of the triangular array of their tungsten bridging oxygens on their surfaces which resemble metal oxide surfaces. On the other hand, ^{183}W nuclear magnetic resonance has proven to be a very good tool for determining the overall symmetry and structure of such polytungstates. Numerous efforts have been undertaken to predict a confident assignment of each tungsten line and to study the electronic changes induced on the polytungstate anion shell in the 1–11 series by the introduction of heteroelements such as transition metals. We show that only *direct* proofs of the tungsten–tungsten connectivities allow an unambiguous conclusion, in contradiction with *all* the actually proposed methods. The *direct* tungsten connectivity is furnished by 2-dimensional ^{183}W NMR on tungsten satellites (COSY and 2D INADEQUATE). The results obtained on $Li_7PW_{11}O_{39}$, $Na_7PW_{11}O_{39}$, $Na_8SiW_{11}O_{39}$, and $Na_5PPbW_{11}O_{39}$ invalidate previously published conclusions.

The importance of heteropolytungstates as key compounds for modelizing the catalytic behavior of metal oxides is well recognized.[1] Thus, the precise knowledge of their spatial and electronic structure is of prime interest. The use of modern single-crystal X-ray diffractometers has allowed the chemist to get a clear static picture for some of these polytungstates. However, in the solid state, the anions are very often found in a statistical distribution between several positions, depending upon the space group symmetry, precluding any quantitative conclusions. As an example, in the so-called Keggin series (1–12 heteropolyanions), the solid salts containing medium sized alkaline cations (K^+, Rb^+, or NH_4^+) associated with $XZW_{11}O_{40}H_n^{(14-x-z-n)-}$ anions[2] have a face centered cubic (or disordered single cubic) structure with 7 to 9 anionic charges, a quadratic structure with 5 to 7 anionic charges, or a hexagonal structure with 4 to 5 charges,[3] although the anion itself shows a low C_s molecular symmetry.

On the other hand, despite its low receptivity (5.89×10^{-2} compared to ^{13}C), tungsten-183 nuclear magnetic resonance is a method of choice for studying the polytungstates series. The very sharp line of the ^{183}W spectra allows the $^nJ_{w-x}$ couplings to be detected easily, and the chemical shifts are very sensitive to electronic or structural changes across the tungsten shell as demonstrated in the pioneering work of Baker et al.[4,5] Actually, the availability of high-field instruments has considerably lowered the barrier of sensitivity, allowing the recording of ^{183}W spectra in a very reasonable time (1–4 h for 0.8–0.4 M solutions).

The chemical shift anisotropy mechanism which may have broaden the tungsten lines too much seems not to be operative for polytungstates under these high-field recording conditions, and several papers have already been published on the study of the symmetry,[6] the isomerism,[7] or fluxionnal behavior[8] of polytungstates. In fact, the NMR spectrum gives not only a clear picture of the overall symmetry (or symmetrizing processes) *in solution* but also a qualitative estimation of the mean electronic charge distribution around each tungsten site through the chemical shifts values. But, if one wants to go deeper into the study of subtle electronic changes across the tungsten shell, it is clear that a precise assignment of *each* tungsten resonance is a prerequisite before some conclusions can be drawn from a comparison in the changes in the ^{183}W chemical shift values. This statement is clearly exemplified within the XZW_{11} series in which the stable α isomer forms a very interesting class of model compounds because of the numerous combinations of both the X and Z elements.[2] Figure 1 shows an idealized representation of a XZW_{11} anion, and Figure 2 exemplifies the dramatic change in the ^{183}W spectrum of the X–Z isomers $GaGe(OH)W_{11}O_{39}^{6-}$ and $GeGa(OH)W_{11}O_{39}^{6-}$ where the Ga and Ge atoms are quasi-isoelectronic. These 1:2:2:2:2:2 spectra confirm the C_s symmetry of the anions and the W_6 resonance can be unambiguously attributed to the smaller peak in both spectra. However, it is clear that no other assignment can be made a priori for the five remaining resonances on the grounds of their chemical shift values. Klemperer et al.[9] proposed to relate the chemical shift values to the X oxidation state by postulating that the overall anionic charge influences the electron density around the W's and hence their nuclear shielding.

Very recently Baker[10] found a very good correlation between ^{183}W chemical shifts and the wavelength of the lowest energy optical absorption in a α-XW_{12} series. He notes also in this paper that the introduction of a quadrupolar Z nuclide ($Z = V^{5+}$) substituting one or more W^{6+} atoms broadens substantially the lines of the adjacent tungsten sites; this broadening coupled with the measured values of $^2J_{W-O-P}$ allows him to propose a partial assignment of the ^{183}W spectra of α-$P_2W_{17}O_{61}^{10-}$, α-$P_2W_{17}VO_{62}^{10-}$, $SiW_{11}O_{39}^{8-}$, and $PW_{11}O_{39}^{7-}$.

We shall show in this paper that very great care has to be taken with both methods[9,10] to avoid erroneous conclusions. In fact, an unambiguous strategy has been proposed recently for a full assignment of the tungsten-183 spectra of heteropolytungstates,[7] based on the homonuclear $^2J_{^{183}W-O-^{183}W}$ couplings which give rise

† Bruker Spectrospin.
‡ Université des Sciences et Techniques du Languedoc.

(1) Baker, L. C. W. "Advances in the Chemistry of Coordination Compounds"; Kirschner, Ed.; MacMillan: New York, 1961; p 604. Pope, M. T.; Dale, B. W. O. *Rev. Chem. Soc.* **1968**, *22*, 257.
(2) We use the abbreviated form XZW_{11} throughout this paper with X = B, Al, Si, Ge, P, As... (tetrahedral site) and Z = transition or main group metallic ion (octahedral site).
(3) Tourné, C. M.; Tourné, G. F. *C. R. Hebd. Seances Acad. Sci., Ser. C* **1968**, *266*, 1363. Evans, H. T. J. *Perspect. Struct. Chem.* **1971**, *4*, 1. Weakley, T. J. R. *J. Chem. Soc., Dalton Trans.* **1973**, 341.
(4) Acerete, R.; Hammer, C. F.; Baker, L. C. W. *J. Am. Chem. Soc.* **1979**, *101*, 267.
(5) Acerete, R.; Harmalker, S.; Hammer, C. F.; Pope, M. T.; Baker, L. C. W. *J. Chem. Soc., Chem. Commun.* **1979**, 777.
(6) Jeannin, Y.; Martin-Frère, J. *J. Am. Chem. Soc.* **1981**, *103*, 1664.
(7) Lefebvre, J.; Chauveau, F.; Doppelt, P.; Brevard, C. *J. Am. Chem. Soc.* **1981**, *103*, 4583.
(8) Sethuraman, P. R.; Leparulo, M. A.; Pope, M. T.; Zonnevijlle, F.; Brevard, C.; Lemerle, J. *J. Am. Chem. Soc.* **1981**, *103*, 7665.
(9) Gansow, O.; Ho, R. K. C.; Klemperer, W. G. *J. Organomet. Chem.* **1980**, *187*, C 27.
(10) Acerete, R.; Hammer, C. F.; Baker, L. C. W. *J. Am. Chem. Soc.* **1982**, *104*, 5384.

0002-7863/83/1505-7059$01.50/0

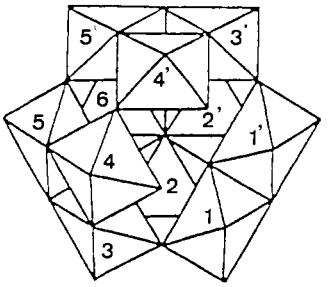

Figure 1. Spatial representation of a XZW_{11} heteropolytungstate. Tungsten atoms are labeled according to Figures 4, 5, and 7 and are located at the center of each oxygen octahedron. For the sake of clarity, the X (central) and Z (edge) atoms have been removed.

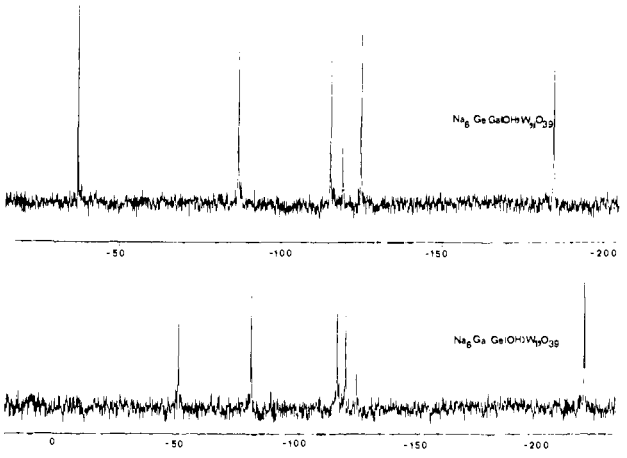

Figure 2. 10.421-MHz tungsten NMR spectra of $Na_6GeGa(OH)W_{11}O_{39}$ and $Na_6GaGe(OH)W_{11}O_{39}$ in D_2O: 303 K, 15 000 scans, reference WO_4^{2-} 2 M in D_2O.

to a fine structure at the foot of each tungsten line (14.27% of the main peak). Interestingly enough, a clear-cut differentiation between "intra-group", edge-linked WO_6 octahedron couplings ($^2J_{^{183}W} \sim 8$ Hz) and "extra-group", corner-linked WO_6 octahedron couplings ($^2J_{^{183}W} \sim 20$ Hz) exists, and this finding has already initiated some interresting studies.[11] However, it may happen that some of these satellites will be hidden in the foot of the main peaks because of spinning artifacts, overlapping resonances, or simply too large a temperature coefficient ($\Delta\delta/K$) for the ^{183}W resonances of the compound under study. Indeed, the use of two-dimensional tungsten NMR on these satellites practically eliminates all the above-mentioned drawbacks and is a very powerful tool for enabling one to get in *one experiment* the desired chemical shifts *and* the connectivity pattern for all the tungsten sites. The two-dimensional NMR sequences that have been used in this work belong to the COSY 90 type sequence[12a,b] and the 2D INADEQUATE type sequence.[12a,13] The COSY sequence is actually widely employed in proton NMR and allows one to relate, within a coupled spectrum, each pair of coupled spins. The 2D INADEQUATE sequence, via a double quantum coherence transfer, allows one to detect low abundance, coupled satellite doublets with elimination of the central peak.

Its application has been directed only toward ^{13}C,[14] but this paper proves, if necessary, that inorganic chemistry will certainly gain a real bonus from such NMR techniques. Indeed, many of the magnetically active spin 1/2 isotopes like ^{29}Si, ^{117}Sn, ^{119}Sn, etc..., have a natural abundance that is greater than the ^{13}C one by a factor ranging from 4 to 15, and one can consider them as potential candidates for these two-dimensional experiments.

Experimental Section

Preparation and Identification of Compounds. The sodium undecatungstophosphate is prepared with a new direct procedure, following the stoechiometric ratio

$$11WO_4^{2-} + HPO_4^{2-} + 17H^+ \rightarrow PW_{11}O_{39}^{7-} + 9H_2O$$

0.22 mol (72.5 g) of sodium tungstate dihydrate and 0.02 mol (2.84 g) of anhydrous disodium hydrogenophosphate are dissolved in 150–200 mL of water. The solution is heated to 80–90 °C and titrated exactly with concentrated nitric acid with vigorous stirring to pH 4.8. The volume is then reduced to half by evaporation and the heteropolyanion separated in a dense lower layer by liquid–liquid extraction with 80–100 mL of acetone. The extraction is repeated until the acetone extract shows no nitric ions (ferrous sulfate test).

The solid sodium salt is obtained as the hydrate ($15–20H_2O$) by evaporation to dryness (in air) of the acetone extracts. Better than with elemental analysis, the compound is characterized by its UV spectrum, the 1/1 complex formation with Co^{2+} and VO^{2+} ions, and the X-ray powder pattern of the quadratic derived potassium salt (precipitated by addition of a saturated methanolic solution of 1:1 potassium acetate–acetic acid to an aqueous solution of the sodium salt).

The lithium undecatungstophosphate is prepared from the potassium salt by cationic exchange on Li^+-form resin (Amberlite IR 120) until the solution shows no reaction with tetraphenylborate. This solution is evaporated to dryness and the product characterized like the sodium salt.

The lead(II) undecatungstophosphate is prepared as its potassium salt first. Potassium undecatungstophosphate reacts with Pb^{2+} (nitrate or acetate) in a 1:1 ratio. The reaction product is recrystallized twice in CO_2-free water. The very soluble sodium salt is obtained by treatment on a Na^+ cationic exchanger. Evaporation to dryness gives a vitreous solid with a lead/tungstophosphate ratio unchanged.

The sodium undecatungstosilicate is prepared and characterized by the same procedures as the sodium undecatungstophosphate (with sodium monosilicate in 2% excess instead of sodium phosphate and a $16H^+/11WO_4^{2-}$ ratio).

The preparation of the potassium salt of $GeGaW_{11}$ and $GaGeW_{11}$ has been described previously.[15] The corresponding sodium salts are obtained by cationic exchange on Na^+-form resins (Amberlite IR 120) and evaporation.

The preparation of undecatungstogallate has been described by Rollins[16a] and Zonnevijlle.[16b] The sodium salt also is obtained by a direct method: dropwise addition of a 1 M gallium nitrate solution (10 mL, 0.01 mol) to a boiling solution of sodium tungstate (36.3 g, 0.11 mol in ~60 mL of water) and acetic acid (6 g, 0.10 mol) with vigorous stirring. The final pH is ~8.5. The pure sodium undecatungstogallate precipitates by adding solid sodium acetate (~20 g) to a warm clear solution (filtered if cloudy) and cooling to room temperature. It is filtered, washed with methanol, and dried in air. A second batch is prepared, and the pure cubic potassium salt is precipitated by addition of potassium acetate and transformed into the sodium salt by cationic exchange in aqueous solution and evaporation to dryness.

The two sodium salts give the same characteriziation test and the same ^{183}W NMR spectra.

Nuclear Magnetic Resonance. The NMR spectra were recorded with a Bruker WM 400 spectrometer equipped with a multinuclear accessory and a 10-mm digital VSP probe covering a frequency range from ^{109}Ag to ^{31}P (2D experiments) or with a Bruker WM 250 fitted with a 15-mm multinuclear probe. The sample temperature was in all cases stabilized with a BVT 1000 unit. The ^{183}W 90° pulse values were 35 μs on the WM 400 and 80 μs on the WM 250. The COSY[12a] experiments were run as 256 × 1 K spectra (960 scans each) with "negative" (N) peak type selection and appropriate phase cycling to allow for quadrature detection in both dimensions. The sequence is written as follows:

$$(t_1\text{-}90_{\phi_1}{}^0\text{-}t_2\text{-}90_{\phi_2}{}^0\text{-AQT})n$$

with t_1 = relaxation delay such as AQT + t_1 = 0.5 s, t_2 = incrementable delay, $\phi_1 = x\bar{x}\bar{x}xy\bar{y}\bar{y}y$, $\phi_2 = xy\bar{x}\bar{y}y\bar{x}\bar{y}x\bar{x}\bar{y}xy\bar{y}xy\bar{x}\bar{x}$, where ϕ_1 and ϕ_2 are pulse phase cycles in which x, $\bar{x}$, y, $\bar{y}$ represent the phase of the exciting radio frequency pulses with respect to the rotating frame axis for each scan (x, x; $-x$, y; $-x$, $-x$, etc...), and n is the total number of scans (a multiple of 16).

(11) Domaille, P. J.; Knoth, W. H. *Inorg. Chem.* **1983**, *22*, 818. Knoth, W. H.; Domaille, P. J.; Roe, D. C. *Ibid.* **1983**, *22*, 198.

(12) a) Bax, A. "Two-Dimensional Nuclear Magnetic Resonance in Liquids"; Delft University Press: 1982. (b) Bax, A.; Freeman, R.; Morris, G. *J. Magn. Reson.* **1981**, *42*, 164.

(13) Bax, A.; Kempsell, S. P.; Freeman, R. *J. Magn. Reson.* **1980**, *41*, 349. Bax, A.; Freeman, R.; Frenkiel, T. A.; Levitt, M. H. *Ibid.* **1981**, *43*, 478.

(14) Jacquesy, R.; Narbonne, C.; Hull, W. E.; Neszmelyi, A.; Luckas, G. *J. Chem. Soc., Chem. Commun.* **1982**, 402.

(15) Zonnevijlle, F.; Tourné, C. M.; Tourné, G. F. *Inorg. Chem.* **1982**, *21*, 2742. Schouten, A. Thèse d'Etat, 1980, U.S.T.L. Montpellier.

(16) (a) Rollins, O. W. *J. Inorg. Nucl. Chem.* **1971**, *33*, 75. (b) Zonnevijlle, F. Thèse d'Etat 1976 U.S.T.L. Montpellier.

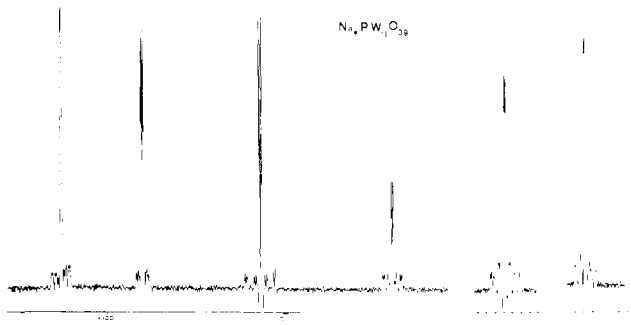

Figure 3. 16.67-MHz tungsten NMR spectrum of $Na_7PW_{11}O_{39}$ in D_2O (1 M): 333 K, 16 000 scans, reference WO_4^{2-} saturated in D_2O (δ +38 from WO_4^{2-} 2 M in D_2O). The satellite peaks from the $^2J_{W-O-W}$, together with the $^2J_{W-P}$ couplings listed in Table I, are clearly visible after a Gaussian deconvolution of the F.I.D.

Table I[a]

W	Intensity	$^2J_{W-O-W}$ (Hz) A	B	C	D	E	F	$^2J_{W-O-P}$ (Hz)
(5) A	2	−97.3ppm	5.6	–	16.8	9.6	–	0.9
(4) B	2	5.6	−10.2	–	–	10.1	–	1.7
(1) C	2	–	–	−108.9	–	27.8	9.8	2.1
(6) D	1	16.8	–	–	−116.6	–	6.6	1.7
(3) E	2	9.6	10.1	27.8	–	−13.2	19.6	1.3
(2) F	2	–	–	9.8	6.6	19.6	−152.1	1.1

[a] Chemical shifts (±0.1 ppm), $^2J_{W-O-W}$, and $^2J_{W-O-P}$ (±0.3 Hz) for $Na_7PW_{11}O_{39}$(aq) (temperature 318 K).

The 2D INADEQUATE experiments were run as 128 × 1 K spectra (1536 scans each) with "positive" (P) type selection and a 32-step phase cycling scheme that allows for quadrature detection in both dimensions. The sequence is written as:

$$(t_1\text{-}90_{\phi_1}{}^0\text{-}\tau\text{-}180_{\phi_2}{}^0\text{-}\tau\text{-}90_{\phi_1}{}^0\text{-}t_2\text{-}90_{\phi_3}{}^0\text{-AQT}_{\phi_4})n + (t_1\text{-}90_{\phi_1}{}^0\text{-}\tau\text{-}180_{\phi_2}{}^0\text{-}\tau\text{-}45_{\phi_5}{}^0\text{-}90_{\phi_1}{}^0\text{-}t_2\text{-}90_{\phi_3}{}^0\text{-AQT}_{\phi_6})n$$

with t_1 = relaxation delay such as AQT + t_1 = 0.5 s, t_2 = incrementable delay, τ = double quantum coherence transfer time = $(2n + 1)/4J_{W-W}$ = 10 ms, $\phi_1 = (x)_8(y)_8(\bar{x})_8(\bar{y})_8$, $\phi_2 = (x\bar{x})_4(y\bar{y})_4$, $\phi_3 = (x)_2(y)_2(\bar{x})_2(\bar{y})_2$ with all phases incremented by 90° three times, $\phi_4 = (Rx)_2(R\bar{y})_2(R\bar{x})_2(Ry)_2$ with all phases incremented by 90° three times, $\phi_5 = (\bar{y})_8(x)_8(y)_8(\bar{x})_8$, and $\phi_6 = (R\bar{y})_2(R\bar{x})_2(Ry)_2(Rx)_2$ with all phases incremented by 90° three times. ϕ_1, ϕ_2, ϕ_3, and ϕ_5 are again associated with the radio frequency pulse phases for each scan. ϕ_4 and ϕ_6 represent the receiver phase during the acquisition period. The total number of scans n is then a multiple of 32. Reference 12a will give the interested reader a very good theoretical and practical introduction to these two-dimensional NMR techniques, the above described pulse sequences being available as standard microprograms on any commercial spectrometer. A typical running time for each experiment is approximately 30 h. Negative chemical shift values indicate a low-frequency (high-field) shift with respect to the reference compound.

For all the polytungstate studies, the chemical shift anisotropy mechanism, if negligible to broaden the lines as indicated before, was sufficient to bring the ^{183}W T_1's in the range of 0.8–1 s, allowing a short recycling time for the 2D experiments. This situation has been noted already for rhodium compounds in 1D experiments.[17]

Results

Figure 3 shows the 16.6-MHz ^{183}W spectrum of $Na_7PW_{11}O_{39}$(aq). Its NMR parameters are gathered in Table I.

Figure 4 represents a COSY experiment on $Na_7PW_{11}O_{39}$ and $Li_7PW_{11}O_{39}$ as a contour plot. One has to remember that he is looking at homonuclearly coupled spin systems that amount to only 14% of the main central peak and hence the appearance of these central peaks along the diagonal chemical shift line of the contour plot with a much bigger intensity than the off-diagonal responses. However, the satellite peaks (see Figure 3) give rise to a clear COSY pattern from which a complete connectivity map

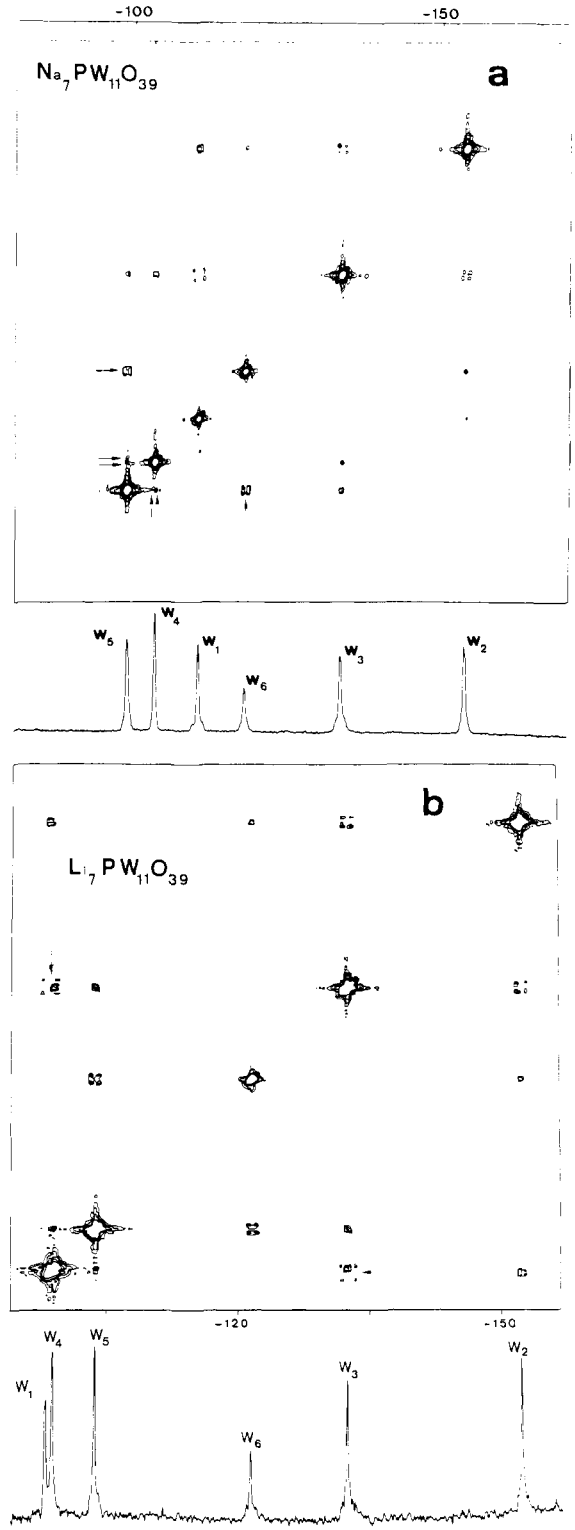

Figure 4. 16.67-MHz, ^{183}W 2D COSY 90 contour plot of $PW_{11}O_{39}^{7-}$ (see the Experimental Section for recording conditions). (a) $Na_7PW_{11}O_{39}$ (303 K, 1 M in D_2O): The coupled tungsten sites are easily detected via their "square shaped pattern" as indicated for W_5 and W_6 (arrows). Note the selectivity of the method for W_5 and W_4 (double arrows). (b) $Li_7PW_{11}O_{39}$ (308 K, 1.2 M in D_2O): The reversal of the W_1 and W_5 resonances is unambiguously detected when compared to $Na_7PW_{11}O_{39}$, showing the influence of the lithium cation in the structure of the PW_{11}^{7-} moiety. Note again the selectivity of the method to discriminate between the connectivity of the two overlapping W_1 and W_4 resonances with W_3 (arrow).

(17) Cocivera, M.; Ferguson, G.; Lenkinski, R. E.; Szczecinski, P. *J. Magn. Reson.* **1982**, *46*, 168.

Table II. ^{183}W Chemical Shifts of $Na_7PW_{11}O_{39}$, $Li_7PW_{11}O_{39}$, $Na_8SiW_{11}O_{39}$, $Na_5PPbW_{11}O_{39}$, and $Na_9GaW_{11}O_{39}$

compd (molarity, temp, D_2O)		$-\delta$ (Wi, $^2J_{W-O-P}$ (Hz))
$Na_7PW_{11}O_{39}$[a] (1 M, 303 K)		97.3 (W5, 0.9); 102 (W4, 1.7); 108.9 (W1, 2.1); 116.6 (W6, 1.7); 132 (W3, 1.3); 152.1 (W2, 1.1)
$Li_7PW_{11}O_{39}$[a] (1.3 M, 308 K)		98.1 (W1, 1.76); 98.8 (W4, 1.76); 103.6 (W5, 0.88); 121.4 (W6, 1.47); 132.4 (W3, 1.17); 152.2 (W2, 1.17)
$Na_8SiW_{11}O_{39}$[a,b] (0.8 M, 303 K)		100.8 (W5); 116.1 (W1); 121.3 (W6); 127.9 (W4); 143.2 (W3); 176.1 (W2)
$Na_5PPbW_{11}O_{39}$[a] (0.8 M, 333 K)		74.4 (W1, 2.20); 82.7 (W4, -); 102.8 (W5, 0.95); 111.5 (W6, 1.47); 127.4 (W3, 1.10); 146.3 (W2, -)
$Na_9GaW_{11}O_{39}$[c] (0.6 M, 303 K)	a species	16.2 (W_6); 101.2; 126.9; 133.8; 137.3; 155.9
	b species	67.4, 81.3; 97.1; 119.2; 125.5; 185.0

[a] Reference WO_4^{2-} saturated in D_2O (WO_4^{2-} 1 M in D_2O: -38 ppm). [b] A second system (~9% of the main one) is detectable at δ: -139.8; -142.1; -144.7; -145.7; -166.7, the 6th peak is certainly hidden under one of the main peaks. [c] Reference WO_4^{2-} 1 M in D_2O.

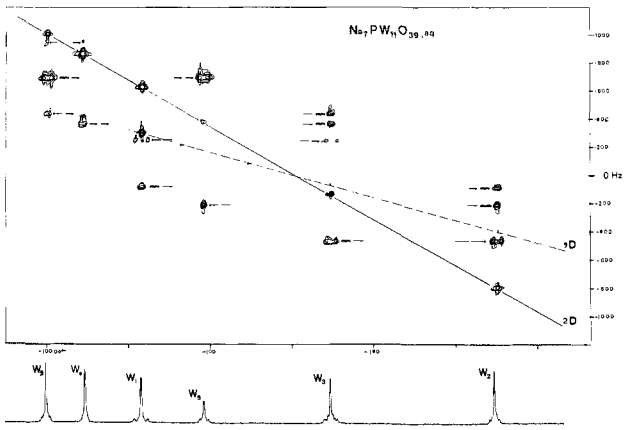

Figure 5. 16.67-MHz ^{183}W 2D INADEQUATE contour plot of $Na_7PW_{11}O_{39}$(313 K). The tungsten connectivities are easily detected with respect to the diagonal (slope -2). The peaks lying on this line come from an imperfect refocusing scheme. Note the clean elimination of each central, non-coupled, 1D tungsten line (residues lie on the line of the slope -1).

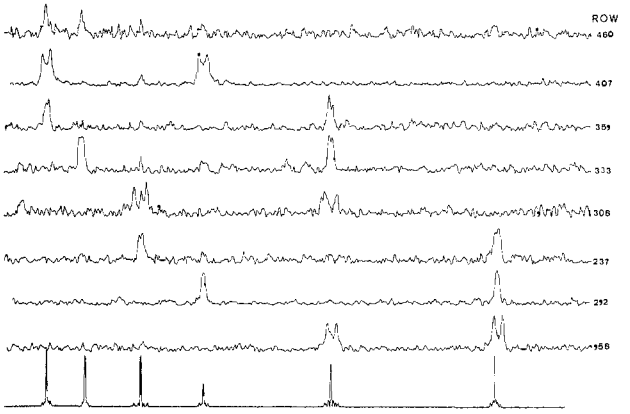

Figure 6. Plot of each matrix row of the 2D experiment of Figure 5, whose number is equal to ($\delta_{W_i}^{carrier} + \delta_{W_j}^{carrier}$).

can be sorted our for each tungsten atom is one remembers (see Figure 1) that in the XZW_{11} series W_1 "sees" W_3 and W_2 (plus Z); W_2 "sees" W_1, W_3, and W_6; W_3 "sees" W_1, W_2, W_4 and W_5; W_4 "sees"W_3 and W_5 (plus Z); W_5 "sees"W_3, W_4, and W_6; and W_6 "sees" W_5 and W_2.

The identification of W_6 is straightforward due to its 1:2 intensity compared with the five other peaks. This W_6 tungsten couples *without any assumption* only with W_5 and W_2. $^2J_{W_6-W_5}$ is an "extra-group" coupling, and $^2J_{W_6-W_2}$ is an "intra-group" coupling. Thus, $^2J_{W_6-W_5} \gg {}^2J_{W_6-W_2}$,[7] and this coupling pattern should be reflected on the COSY plot. This is indeed the case (see Figure 4), and an immediate identification of W_5 and W_2 follows. The three remaining lines are then assigned very easily.

The method can be refined by using a 2D INADEQUATE[12a,13] sequence, (see Experimental Section), which, as a contour plot, (a) eliminates the 1D central peaks (residues along a line of slope -1) and (b) maps out each pair of coupled satellite peaks symmetrically with respect to the diagonal (slope -2).

Figure 5 shows such an experiment on $Na_7PW_{11}O_{39}$(aq) which very nicely confirms the COSY result and the tungsten connectivities. A plot of the 2D matrix rows, the number of which are equal to the algebric sum (in Hz) of the shift of each pair of coupled peaks with respect to the carrier frequency, visualizes this connectivity (Figure 6).

Interestingly enough a small coupling is detected with both methods between W_5 and W_4, which was barely visible on the 1D spectrum (Figures 4a and 5). On the other hand, both 2D techniques detect a clear-cut quadratic connectivity for tungsten W_3 in $Na_7PW_{11}O_{39}$, although the 1D spectrum shows only a three-coupling pattern with slightly different intensities.

Finally, Figure 7 represents a 2D INADEQUATE experiment run on $Na_5PPbW_{11}O_{39}$(aq) with the corresponding assignment for each tungsten resonances. One can clearly see the inversion, hardly predictable when compared to $Na_7PW_{11}O_{39}$(aq) for the chemical shifts of W_1 and W_5 due to the influence of the lead atom[18] and discussed in the next section.

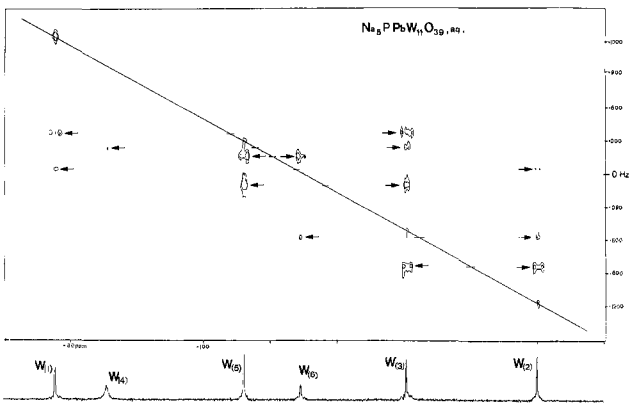

Figure 7. 16.67-MHz ^{183}W 2D INADEQUATE contour plot of $Na_5PPbW_{11}O_{39}$ (333 K, 0.8 M in D_2O). (Same acquisition parameter as Figure 5).

Discussion

We have then in hand a direct proof of the tungsten–tungsten connectivities that allows us to fully discuss the method and the assignments suggested by Baker et al.[10] for the 11 tungsto derivatives.

Table II summarizes the complete assignment of the ^{183}W spectra of $Li_7PW_{11}O_{39}$, $Na_7PW_{11}O_{39}$, $Na_8SiW_{11}O_{39}$, and $Na_5PPbW_{11}O_{39}$ confirmed with both COSY and 2D INADEQUATE experiments.

In fact, our findings strongly weaken their general model for these 11 tungsto derivatives in which the two most deshielded tungsten lines are attributed to the two pairs of W's nearest to the vacancy (W_1 and W_4). These lines, clearly, can also originate from W_5, W_4 ($Na_7PW_{11}O_{39}$ or W_5, W_1 ($Na_8SiW_{11}O_{39}$). On the other hand, our method permits one to precisely attribute all the resonances, which were not attributed in Baker's paper. On the contrary, our $PPbW_{11}^{5-}$ assignment (Figure 7, Table II) is in

(18) Tourné, G.; Tourné, C. M.; Schouten, A. *Acta. Crystallogr., Sect. B* **1982**, *B38*, 1414.

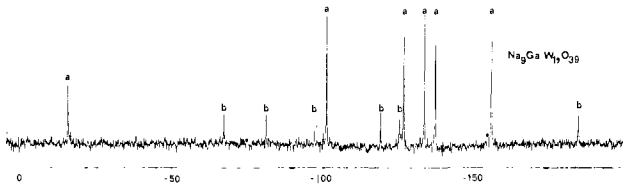

Figure 8. 10.421-MHz ^{183}W spectrum of $Na_9GaW_{11}O_{39}$ (303 K, 0.6 M in D_2O, 20 000 scans). One clearly sees the two imbricated 1:2:2:2:2:2 patterns; a peaks are attributed to $GaNaW_{11}^{8-}$ and b peaks to GaW_{11}^{9-}.

agreement with his hypothesis, and one could note the width of the W_4 line (see Figure 7). This broadening should indicate some kind of dynamic process that this W_4 tungsten is taking part in (^{207}Pb in a spin 1/2 nuclide which eliminates a quadrupolar broadening on W_4). This line also shifts strongly with temperature variations. In fact, our results do substantiate the hypothesis of Tourné[19] and Contant,[20] who suggested that alkaline or alkaline-earth cations (C) can be complexed by lacunary type heteropolyanions $X\square W_{11}$, giving rise to a XCW_{11} type structure, which is no longer a true lacunary type structure. The W chemical shift values of these XCW_{11} polytungstate anions then reflect the overall electronic change and spatial deformation due to the inclusion of the C cation into the vacancy. This assertion is strengthened by the change in the ^{183}W spectrum of $PW_{11}O_{39}^{7-}$ that occurs by simply replacing the sodium cation by a lithium cation. In $Na_7PW_{11}O_{39}$, the two most deshielded resonances W_5 and W_4 are well separated when the ^{183}W spectrum of $Li_7PW_{11}O_{39}$ shows a near coalescence of these two lines with an inversion of W_5 and W_1 (Figure 4a,b and Table II) which indicates a real "intramolecular" participation of the counterion in the polytungstate anionic structure as detected[19,20] with other methods. On the other hand, the ^{183}W spectra of the sodium salts of SiW_{11}, GeW_{11}, or GaW_{11} (0.6–1.2 M in D_2O), contrary to Na_7PW_{11}, clearly show a double system of six 1:2:2:2:2:2 peaks in a different overall ratio depending upon the X element.

Figure 8 exemplifies the $Na_9GaW_{11}O_{39}$ spectrum. The b peaks are tentatively attributed to the lacunary GaW_{11}^{9-} anion, with the a peaks representing the $GaNaW_{11}^{8-}$ species. This double system was certainly not detected by Baker et al.[4] for $Na_8SiW_{11}O_{39}$ because of the low percentage of the b species (see Table II). We could not detect such a XCW_{11} species by ^{23}Na NMR on $Na_7PW_{11}O_{39}$(aq) or $Na_8SiW_{11}O_{39}$(aq), which show only one resonance (δ 0.3 from NaCl saturated in D_2O, $\Delta\nu_{1/2}$ = 160 Hz). This fact indicates that the sodium cation is probably in fast exchange on the NMR time scale between the free and complexed sites (there is no noticeable change in the resonance width when going from 5.87 to 9.4 T). We also recorded the[7] Li (at 9.4 T) spectrum of $Li_7PW_{11}O_{39}$(aq), but again only one resonance was found ($\delta \sim +0.5$ from LiCl 1 M in D_2O, $\Delta\nu_{1/2}$ = 2 Hz), confirming the situation detected for the sodium salts. Nevertheless, our results can be rationalized in the following way:

The introduction of a Z heteroelement in the vacancy of $X\square W_{11}$ polytungstates modifies not only the chemical shifts of the adjacent tungsten atoms but also the chemical shift of the remote tungsten atoms, following the electronic *and* spatial modifications induced by this Z element (Z net charge and size), and no indirect rule can be set to predict this chemical shift change.

In the so called lacunary series $X\square W_{11}$, the vacancy is certainly filled by one of the corresponding countercations. The difference in the chemical shifts of the W_5, W_1, and W_4 tungstens between $Li_7PW_{11}O_{39}$(aq), $Na_7PW_{11}O_{39}$(aq), and $Na_8SiW_{11}O_{39}$(aq) then can be explained if we note that the ionic radius is bigger for Na^+ than for Li^+. The small lithium, electron poor, ion deeply encaped into the cavity acts as a symmetrizing agent for the (W_1–W_4–W_5) part of the polytungstate moiety rendering the W_1 and W_4 tungsten atoms nearly equivalent. On the contrary, the encapsulated sodium cation, bigger in size, distorts the tungstate structure such as to completely split and shift the W_1, W_4, and W_5 lines. The inversion of the W_5 and W_1 resonances observed for $PPbW_{11}^{5-}$ confirms the spatial arrangement of the lead Z atom as observed in the parent component $GaPbW_{11}^{7-}$.[17] The X-ray structure of $GaPbW_{11}^{7-}$ indicates that the lead atom strongly binds only four oxygen atoms with a short Pb–W_1 distance (3.787 Å) and a long Pb–W_4 one (4.062 Å). There is also a clear rejection of the lead atom toward the exterior of the vacancy, and the overall electronic and steric structures of $GaPW_{11}O_{39}^{7-}$ and $PPbW_{11}O_{39}^{5-}$ then paradoxically approach the $PLi(OH_2)W_{11}O_{39}^{6-}$ structure. When comparing the $Na_7PW_{11}O_{39}$ and $Na_8SiW_{11}O_{39}$ spectra, the assignment of the W_5 resonance peak is not inverted. This fact suggests a specific influence of the Na^+ ion complexed by the lacunary heteropolyanion. Note also the unexpected high-frequency shift ("deshielding") of W_5 in both compounds, and note that W_2 is always found at the lowest frequency range ("shielding") (recently observed also in $PTiW_{11}O_{40}^{5-}$ [11]).

Finally, each polytungstate anion *must* be considered as a *unique entity* with its own overall electronic charge and spatial structure, and the distribution of these effects on the ^{183}W chemical shifts can completely reverse the ^{183}W chemical shift assignment, as exemplified in $Na_7PW_{11}O_{39}$ and $Li_7PW_{11}O_{39}$.

Conclusion

^{183}W 2D NMR techniques will certainly, in the near future, prove to be a unique method for studying the heteropolytungstate family. They will give the chemist a direct method for assigning each tungsten resonance and help him to understand the structure and properties of these very important compounds. These 2D methods can be chosen very precisely depending upon the information that is needed. As an example, the sensitivity of the 2D INADEQUATE experiment can be improved by using recently proposed modifications[21] or the COSY information can be selected by fine tuning the transfer period of the sequence to emphasize long-range couplings (COSY 45). Our results are also an obvious pleading for the XZW_{17}, $X_2Z_3W_{18}$, and related series. We hope that the extension of these 2D methods to other low to medium natural abundance, low γ, spin 1/2 isotopes will also be initiated by our paper.

Registry No. ^{183}W, 14265-81-7; W, 7440-33-7; $Na_7PW_{11}O_{39}$, 87261-30-1; $Li_7PW_{11}O_{39}$, 82691-60-9; $Na_8SiW_{11}O_{39}$, 64684-54-4; $Na_5PPbW_{11}O_{39}$, 87281-26-3; $Na_9GaW_{11}O_{39}$, 83698-65-1.

(19) Tourné, G. *Bull. Soc. Chim.* **1982**, *69*, 3.
(20) Contant, R.; Ciabrini, J. P. *J. Chem. Res. Synop.* **1982**, *2*, 50.
(21) Mareci, T. H.; Freeman, R. *J. Magn. Reson.* **1982**, *48*, 158. Turner, D. L. *Ibid.* **1982**, *49*, 175.